Quasiparticle random phase approximation uncertainties and their correlations in the analysis of $0\nu\beta\beta$ decay

Amand Faessler,[1] G. L. Fogli,[2,3] E. Lisi,[3] V. Rodin,[1] A. M. Rotunno,[2,3] and F. Šimkovic[1,4,5]

[1]*Institute of Theoretical Physics, University of Tuebingen, 72076 Tuebingen, Germany*
[2]*Dipartimento Interateneo di Fisica "Michelangelo Merlin," Via Amendola 173, 70126 Bari, Italy*
[3]*Istituto Nazionale di Fisica Nucleare, Sezione di Bari, Via Orabona 4, 70126 Bari, Italy*
[4]*Bogoliubov Laboratory of Theoretical Physics, JINR, 141980 Dubna, Russia*
[5]*Department of Nuclear Physics, Comenius University, Mlynská dolina F1, SK-842 15 Bratislava, Slovakia*

The variances and covariances associated to the nuclear matrix elements of neutrinoless double beta decay ($0\nu\beta\beta$) are estimated within the quasiparticle random phase approximation. It is shown that correlated nuclear matrix elements uncertainties play an important role in the comparison of $0\nu\beta\beta$ decay rates for different nuclei, and that they are degenerate with the uncertainty in the reconstructed Majorana neutrino mass.

I. INTRODUCTION

The search for the neutrinoless mode of double beta decay ($0\nu\beta\beta$),

$$(Z, A) \rightarrow (Z + 2, A) + 2e^-, \tag{1}$$

is being vigorously pursued by several experiments using different (Z, A) nuclei, in order to unravel the Dirac or Majorana nature of neutrinos and their absolute mass scale [1]. In a given candidate nucleus $i = (Z, A)$, light Majorana neutrinos can induce $0\nu\beta\beta$ decay with half-life T_i given by

$$T_i^{-1} = G_i |M_i'|^2 m_{\beta\beta}^2 \tag{2}$$

where G_i is a calculable phase-space factor, M_i' is the $0\nu\beta\beta$ nuclear matrix element (NME), and $m_{\beta\beta}$ is the "effective Majorana neutrino mass,"

$$m_{\beta\beta} = \left| \sum_{k=1}^{3} m_k U_{ek}^2 \right|, \tag{3}$$

where m_k and U_{ek} are the neutrino masses and the ν_e mixing matrix elements, respectively, in standard notation [2]. The NME includes both Fermi (F) and Gamow-Teller (GT) transitions, plus a small tensor (T) contribution [3],

$$M_i' = \left(\frac{g_A}{1.25}\right)^2 \left(M_i^{\text{GT}} + M_i^{\text{T}} - \frac{M_i^{\text{F}}}{g_A^2}\right). \tag{4}$$

In the above expression, g_A is the effective axial coupling in nuclear matter, not necessarily equal to its "bare" free-nucleon value $g_A \simeq 1.25$. With the conventional prefactor $\propto g_A^2$ in Eq. (4), the phase-space G_i becomes g_A-independent. In general, all parametric uncertainties (which may be quite large) are embedded in $|M_i'|$ [4].

It is widely recognized that a convincing case for $0\nu\beta\beta$ decay must involve independent signals in three or more nuclei [1,5]. For instance, if the theoretical NME uncer-

tainties could be roughly expressed in terms of a single nuisance parameter p, then one would need two independent half-life data T_1 and T_2, and two relations as Eq. (2), to fix both p and $m_{\beta\beta}$ (up to degeneracies). A third datum T_3 would overconstrain the system of equations, providing a cross-check of the results [6–8]. A negative check might signal possible new $0\nu\beta\beta$ physics beyond light Majorana neutrinos (barring experimental or theoretical mistakes). Any new $0\nu\beta\beta$ mechanism(s) would then involve at least one more unknown, and thus it might require one or more data ($T_4, T_5, \dots$) for further cross-checks [9–11]. Statistical assessments of the various options demand realistic estimates of experimental and theoretical uncertainties, and the analysis of possible degeneracies which, as we shall see, may play a relevant role.

Recently, there has been significant progress towards the reduction (and a better evaluation) of $0\nu\beta\beta$ theoretical errors. Within the quasiparticle random phase approximation (QRPA) [3], these uncertainties can be largely kept under control by systematically fixing, in each nucleus, the particle-particle strength parameter g_{pp} via two-neutrino double beta ($2\nu\beta\beta$) decay rates. In this way, the dispersion of NME values obtained by varying several QRPA ingredients has been significantly reduced (see [4] and references therein).

However, the estimated NME *variances* do not exhaust the information needed to compare $0\nu\beta\beta$ limits (or signals) in different nuclei: the NME *covariances* are important as well. Nonzero NME covariances have been implicitly recognized in a few works, e.g., by studying the dispersion of NME ratios [8], and by observing that such a dispersion may be smaller than for individual NME [10]. To our knowledge, these observations—implying positive NME correlations—have not yet been sharpened from a statistical viewpoint, despite their relevant consequences for the comparison of $0\nu\beta\beta$ signals. In a nutshell, the main points can be illustrated as follows. If a finite half-

life T_i is measured in a nucleus i, the half-life expected in another nucleus j is

$$T_j = T_i \frac{G_i}{G_j} \frac{|M_i'|^2}{|M_j'|^2}, \qquad (5)$$

within (large) NME uncertainties. From the experimental viewpoint, the "most favorable case" would entail the shortest decay timescale T_j, namely, the smallest $|M_i'|$ and the largest $|M_j'|$. However, if the two NME uncertainties were positively correlated (e.g., via a common normalization factor), opposite changes of $|M_i'|$ and $|M_j'|$ would be unlikely, thus preventing the occurrence of the "experimentally favorable" case. Moreover, a common shift of the NME for *all* nuclei could always be compensated by an inverse shift in $m_{\beta\beta}$ via Eq. (2), leading to a degeneracy between (correlated) theoretical errors and the Majorana neutrino mass.

The purpose of this paper is to explore and discuss these issues in detail. In Sec. II we set our notation and conventions. In Sec. III we present our evaluation of the covariance matrix for the NME in a set of nuclei. In Sec. IV we apply our formalism to relevant cases in the $0\nu\beta\beta$ phenomenology. In Sec. V we summarize our work and discuss future perspectives. An Appendix collects additional details about different theoretical evaluations of G_i and $|M_i'|$.

II. NOTATION AND CONVENTIONS

In the spirit of Refs. [12–14], we shall use logarithms of the main $0\nu\beta\beta$ quantities in appropriate units, namely:

$$\tau_i = \log_{10}(T_i/y), \qquad (6)$$

$$-\gamma_i = \log_{10}[G_i/(y^{-1} \ eV^{-2})], \qquad (7)$$

$$\eta_i = \log_{10}|M_i'|, \qquad (8)$$

$$\mu = \log_{10}(m_{\beta\beta}/eV), \qquad (9)$$

so that Eq. (2) is linearized as

$$\tau_i = \gamma_i - 2\eta_i - 2\mu. \qquad (10)$$

Central values and errors will be denoted as

$$\tau_i = \tau_i^0 \pm s_i, \qquad (11)$$

$$\eta_i = \eta_i^0 \pm \sigma_i, \qquad (12)$$

$$\mu = \mu^0 \pm \delta, \qquad (13)$$

the γ_i having virtually no uncertainties (see however the Appendix for remarks). Experimental measurements of the τ_i's are thus translated into linear constraints on the unobservable quantity μ, once the nuclear matrix elements η_i and their covariances are given.

Linearization through logarithms is appropriate to deal with relatively large NME errors. For instance, a typical "factor of two" uncertainty, $|M_i'| = |M_i'^0| \times (1^{+1.0}_{-0.5})$, entails at least two drawbacks: (i) asymmetric errors are difficult to manage with usual statistical tools (such as least-squares methods); (ii) the unphysical region $|M_i'| < 0$ is hit at twice the lower error. Both drawbacks are avoided by expressing the same "factor of two" uncertainty as $\eta_i = \eta_i^0 \pm 0.30$.

Concerning the quantities $\tau_i = \log_{10}(T_i/y)$, at present there is only one claim for a positive $0\nu\beta\beta$ result by Klapdor *et al.* [15,16] as part of the Heidelberg-Moscow Collaboration: $T_i/y = 2.23^{+0.44}_{-0.31} \times 10^{25}$ at 1σ [16]. We translate this claimed range as

$$\tau_i = 25.355 \pm 0.072 \qquad (1\sigma, i = {}^{76}Ge), \qquad (14)$$

where we have slightly displaced the experimental central value so as to reproduce the 1σ extrema, by construction, with symmetric errors [17]. For $n > 1$, the asymmetric $n\sigma$ ranges $T_i/y = 2.23^{+n\cdot 0.44}_{-n\cdot 0.31} \times 10^{25}$ correspond to the symmetric ranges $\tau_i = 25.355 \pm n \cdot 0.072$ within an acceptable accuracy of 10%, i.e., within about 0.2σ (0.3σ) at the level of 2σ (3σ) ranges.

The above arguments, as well as the advantages of using linear relations [Eq. (10)] and the associated simple statistics (linear propagation of errors, χ^2 methods), lead us to assume approximately gaussian errors on $\log z_i$, rather than on z_i (where $z_i = T_i, |M_i'|$), for the purposes of this work. In the future, a better knowledge of the probability distributions of the z_i's might warrant a different approach, possibly based on more refined statistical tools applicable to generic random variables (maximum likelihood methods, Monte Carlo simulations). However, our main results do not crucially depend on these subtle aspects.

III. NME UNCERTAINTIES AND THEIR CORRELATIONS

In this section we discuss estimates for the nuclear matrix elements η_i, in terms of central values η_i^0, errors σ_i and correlations ρ_{ij}, for a set of eight $0\nu\beta\beta$ candidate nuclei: $i = {}^{76}Ge, {}^{82}Se, {}^{96}Zr, {}^{100}Mo, {}^{116}Cd, {}^{128}Te, {}^{130}Te,$ and ${}^{136}Xe$. We remind that the associated covariance matrix is $cov(\eta_i, \eta_j) = \rho_{ij}\sigma_i\sigma_j$, whose diagonal elements coincide with the variances σ_i^2.

A. Numerical evaluation of QRPA uncertainties

Our estimates are based on a large set of QRPA calculations [4,18] which include $2 \times 2 \times 3 \times 2 = 24$ variants in the input ingredients, namely: (i) two values for the axial coupling: $g_A = 1.25$ (bare) and $g_A = 1.00$ (quenched); (ii) two approaches to short-range correlations (s.r.c.): the so-called Jastrow-type s.r.c., and the unitary correlation operator method (UCOM); (iii) three sizes for the model basis: small, intermediate and large; (iv) two many-body

models: QRPA and its renormalized version (RQRPA). All the 24 variants are supplemented by errors induced by g_{pp} uncertainties (within the experimental $2\nu\beta\beta$ constraints). Concerning NME error estimates, we adopt the same conservative approach as in [18], and define the 1σ range $\eta_i^0 \pm \sigma_i$ as the one embracing the minimum and maximum calculated value of η_i for each nucleus i. These $\pm 1\sigma$ errors are more generous than their formal statistical definition (which would embrace only $\sim 68\%$ QRPA variants, i.e., ~ 16 out of 24). Finally, we calculate the correlation index ρ_{ij} between joint (η_i, η_j) values taken from the same QRPA sample. In all cases, we also include g_{pp}-induced variations.

Our final results for η_i, σ_i and ρ_{ij} are reported in Table I (together with the values of the phase-space factors γ_i, for completeness). Figure 1 shows the same results in graphical form, for each couple of different nuclei, in the plane charted by the coordinates (η_i, η_j). In each panel we show the "1σ error ellipse," centered at (η^0, η_j^0) and with correlation ρ_{ij}; its projection onto a coordinate axis coincide with the $\pm 1\sigma_i$ range defined previously. Also shown in each panel is the set of QRPA calculations used, supplemented by the horizontal and vertical error bars induced by g_{pp} uncertainties (for a total of 24 "crosses" in each plane).

In Fig. 1, the strong, positive correlation among theoretical estimates emerges at a glance. The QRPA calculations are mostly scattered along a primary direction (the ellipse major axis) with positive slope, essentially as a result of variations in the s.r.c. model (either Jastrow, blue, or UCOM, red) and, secondarily, to variations in g_A. There is also some dispersion in the orthogonal direction (ellipse minor axis), which is mainly due to g_{pp} variations. In general, the overall scatter of QRPA is very well captured by the ellipses, with the possible exception of those involving $j = {}^{96}\text{Zr}$, which are somewhat undersampled at low η_j. For this nucleus, the g_{pp} parameter turns out to be extremely close to the so-called QRPA collapse point, the η_j estimates becoming less reliable and more erratic as collapse is approached—leading to large and asymmetric error bars. For other nuclei, g_{pp} is

far from the collapse point and the results are more stable (with smaller and more symmetric g_{pp} errors), as compared to ^{96}Zr. In conclusion, the correlations ρ_{ij} reported in Table I appear adequate to characterize the scatter of QRPA variants, with the only possible exception of ^{96}Zr, whose estimates must be taken with a grain of salt.

We remark that the above estimates, performed within the QRPA, include only known and controllable sources of uncertainties. Some of them are peculiar of QRPA (e.g., g_{pp}), while others are common to any nuclear model (e.g., g_A and the s.r.c.). It is not excluded that future developments in nuclear theory and data may suggest the inclusion of further parametric uncertainties, most notably those related to deformation and to low-lying β^+ strengths.

Indeed, a reliable description of the low-lying β^+ strengths is a challenging task, which calls for some improvement of the QRPA calculations. In fact, the $2\nu\beta\beta$-decay matrix element used to fix the value of g_{pp} is dominated by contributions of low-lying states of the intermediate nucleus. A recent study [19] has shown that a better agreement for contributions of low-lying states to the $2\nu\beta\beta$-decay matrix element can be achieved by adjusting the single-particle energies so as to reproduce experimental occupation numbers of neutron and proton valence orbits in ^{76}Ge and ^{76}Se. For a systematic analysis of this kind of effects one needs more experimental data (measuring the neutron and proton occupancies in particle adding and removing transfer reactions [20], measuring the beta strength distributions in charge-exchange reactions [21], etc.) and further theoretical studies, which go beyond the scope of this paper.

Our results must thus be interpreted as an attempt to quantify conservatively the role of known QRPA uncertainties, which does not exclude that further corrections may be required by future developments in this evolving field of research.

B. Comparison with other estimates and discussion

In Fig. 2 (in the same coordinate planes of Fig. 1) we show our error ellipses at 1, 2 and 3 standard deviations ($\Delta\chi^2 = 1$, 4, and 9, respectively), and superpose the latest

TABLE I.   For each nucleus i, we report the phase-space factor γ_i, the central value of the nuclear matrix error η_i, and the error σ_i, together with the (symmetric) error correlation matrix ρ_{ij}, according to the QRPA estimates in this work. See the text for definitions.

| i | γ_i | η_i^0 | σ_i | correlation matrix ρ_{ij} | | | | | | | |
				^{76}Ge	^{82}Se	^{96}Zr	^{100}Mo	^{116}Cd	^{128}Te	^{130}Te	^{136}Xe
^{76}Ge	25.517	0.635	0.122	1							
^{82}Se	24.870	0.571	0.135	0.978	1						
^{96}Zr	24.550	0.038	0.247	0.518	0.506	1					
^{100}Mo	24.660	0.503	0.162	0.973	0.957	0.491	1				
^{116}Cd	24.622	0.404	0.150	0.961	0.961	0.474	0.965	1			
^{128}Te	26.073	0.534	0.154	0.947	0.968	0.515	0.916	0.930	1		
^{130}Te	24.674	0.498	0.158	0.899	0.927	0.575	0.862	0.870	0.964	1	
^{136}Xe	24.644	0.254	0.187	0.805	0.846	0.663	0.747	0.773	0.898	0.916	1
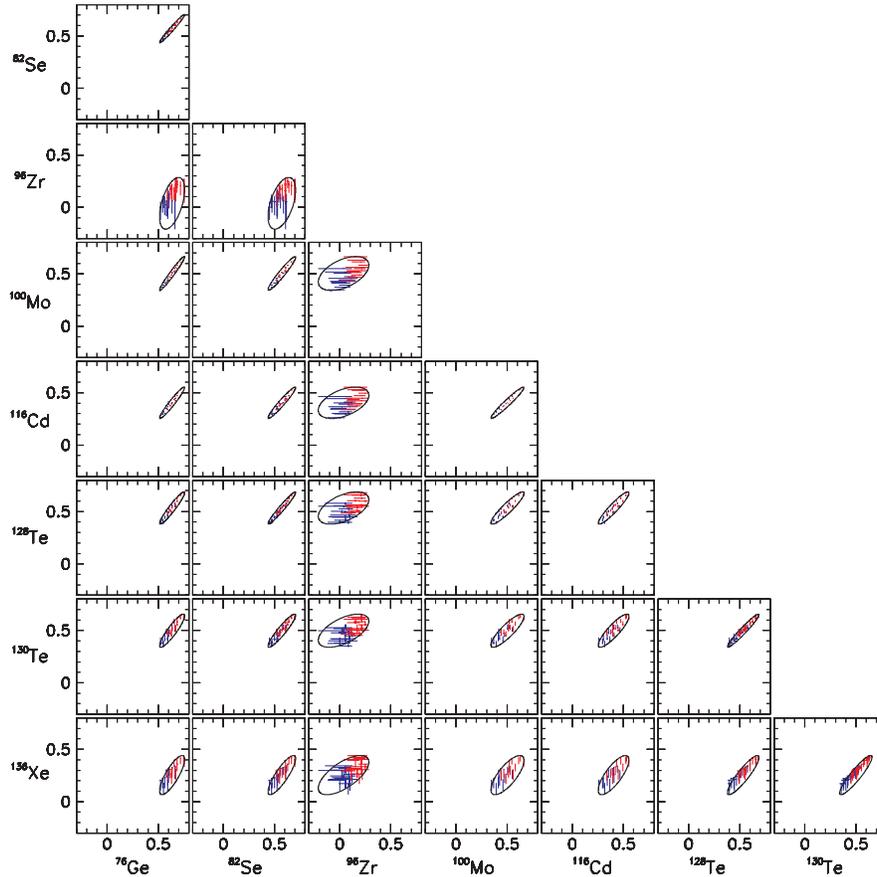
FIG. 1 (color online). Scatter plot of estimated QRPA values for the (logarithms of) nuclear matrix elements (η_i, η_j) for each couple of nuclei (i, j), together with the error bars induced by g_{pp} uncertainties. In each panel, also shown is the 1σ error ellipse, conservatively estimated on the basis of the scatter plots. See the text for details. Color code for s.r.c: blue (Jastrow), red (UCOM).

QRPA results from Ref. [22] (dots) and the latest shell-model results from Ref. [23,24] (stars, for the available nuclei). For each nucleus, these independent η_i evaluations fall within our estimated 3σ range, $\eta_i^0 \pm 3\sigma_i$. Joint estimates of (η_i, η_j) for couples of nuclei appear to be roughly aligned along (or parallel to) the major axis of each ellipse, providing an independent confirmation of positive correlations between the NME. The joint estimates also fall within our 3σ ellipses in most cases, with a few moderate exceptions in some panels of Fig. 2. We refrain, however, from enlarging our errors (or decreasing their correlations), in order to accommodate these few outliers within each 3σ error ellipse. A motivated revision of our estimates should be based on a detailed comparison of our probability distributions with analogous ones from independent calculations—rather than with a few sparse points from the published literature.

Therefore, it would be useful if other theoretical groups in the $0\nu\beta\beta$ field could also present "statistical samples" of NME calculations, as suggested in this work, so as to provide independent estimates of (co)variances for their NME estimates. In fact, our (co)variances cannot be directly applied to other NME evaluations which, in general,

do not share the same set of error sources. In any case, we stress that our evaluation of QRPA uncertainties is conservative enough to cover the most updated, independent NME calculations within $\pm 3\sigma$ for each individual nucleus—see Table VI in the Appendix. Further work is clearly needed to achieve a better convergence among the central values estimated in different models and, possibly, to reduce their associated errors.

Some final remarks are in order. As already mentioned, the high correlation in each panel of Fig. 1 is mainly due to the fact that, if the s.r.c. model or the g_A parameter are varied, all NME tend to either increase or decrease jointly. However, the assumption that g_A is the same in all nuclei may be too strong, as the amount of quenching might change in different nuclei. In particular, we have shown in [25] that, by using more data besides $2\nu\beta\beta$ as additional constraints, the fitted values of g_A is not necessarily constant. Independent variations of g_A in different nuclei would generally weaken the correlations in Fig. 1. Similarly, nucleus-dependent deformations (ignored in this work) might lead to a further spread of errors and to weaker correlations. In general, for any two given nuclei, the more different their physics (in terms of g_{pp}, g_A,
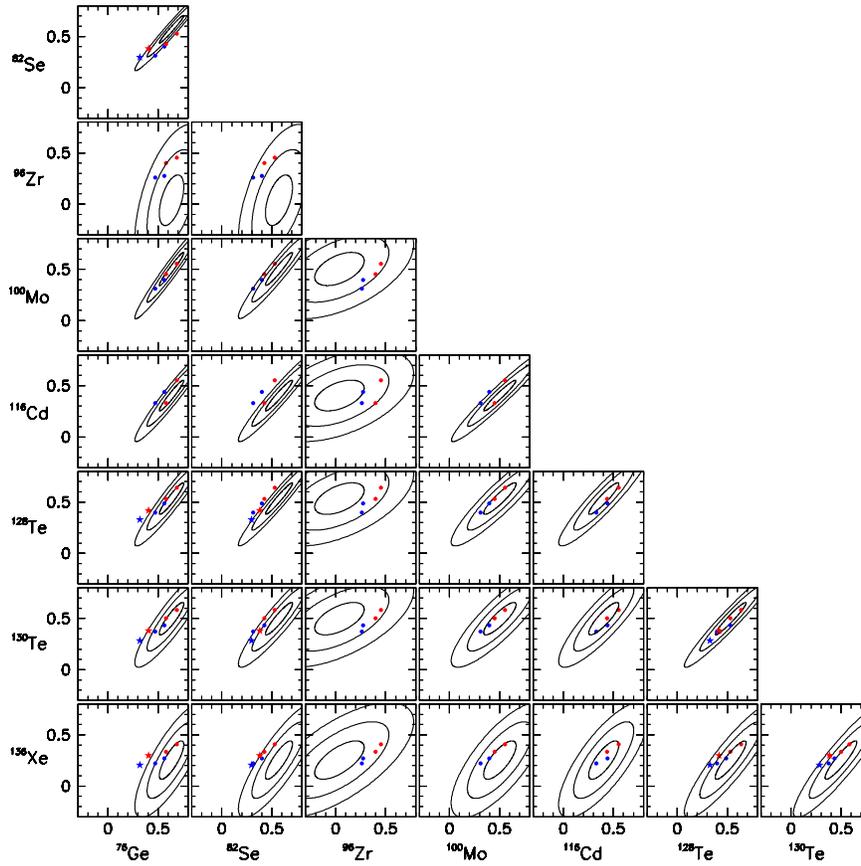
FIG. 2 (color online).   Error ellipses at 1σ, 2σ and 3σ, as derived from Fig. 1 and compared with independent nuclear matrix element calculations from [22] (QRPA, dots) and [23] (shell model, stars). Color code for s.r.c: blue (Jastrow), red (UCOM).

deformation, etc.), the weaker their correlation (in terms of nuclear matrix elements). Our estimated correlations might thus be lowered in the future, should the standard assumptions in QRPA modeling be relaxed in different ways for different nuclei. Despite all these caveats, our ρ_{ij} matrix represents at least a first, approximate attempt to quantify existing correlations of theoretical uncertainties. Neglecting ρ_{ij} altogether would definitely lead to worse approximations.

IV. APPLICATIONS

In this section we apply the previous results to cases of practical interest, in order of increasing complexity.

A. An application not involving correlations

As a first application (not involving correlations), we translate 90% C.L. limits on half-lives into 90% limits on the Majorana neutrino mass. We remind that a two-sided 90% C.L. range corresponds to $\pm 1.64\sigma$ ($\Delta\chi^2 = 2.7$); therefore, the claim in Eq. (14) corresponds to

$$\tau_i = \tau_i^0 \pm 1.64s_i = 25.355 \pm 0.118 \quad (90\% \text{C.L.}, i = {}^{76}\text{Ge}).$$

(15)

and thus to the following 90% C.L. range for μ [as given by Eq. (10)]:

$$\mu \pm 1.64\delta = \frac{1}{2}(\gamma_i - \tau_i^0 \pm 1.64s_i) - (\eta_i^0 \pm 1.64\sigma_i)$$
$$= -0.554 \pm 0.208 \quad (90\% \text{C.L.}, i = {}^{76}\text{Ge}),$$

(16)

where the two errors ($s_i/2$ and σ_i) have been added in quadrature, being uncorrelated. The corresponding preferred range for the Majorana neutrino mass is:

$$m_{\beta\beta}/\text{eV} = [0.17, 0.45] \quad (90\% \text{C.L.}, i = {}^{76}\text{Ge}). \quad (17)$$

The best one-sided 90% C.L. limits for various nuclei have been recently reviewed in [26], in terms of half-lives at 90% C.L. ($\tau_i > \tau_i^{90}$), as reported in Table II. It is worth noticing that, if former data from the Heidelberg-Moscow experiment were interpreted as a limit on (rather than a signal of) $0\nu2\beta$ decay, the 90% C.L. bound on the ^{76}Ge half-life would be 1.9×10^{25} y [33], slightly stronger than the one placed by IGEX [27] in Table II.

The information in Table II can be transformed into 90% C.L. limits of the form $\mu < \mu^{90}$ via the relation

TABLE II.   Best current limits on half-lives at 90% C.L. ($T_i > T_i^{90}$ and $\tau_i > \tau_i^{90}$) for different nuclei i, from [26].

i	T_i^{90}/y	τ_i^{90}	Experiment	Ref.
^{76}Ge	1.6×10^{25}	25.204	IGEX	[27]
^{82}Se	2.1×10^{23}	23.322	NEMO-3	[28]
^{96}Zr	8.6×10^{21}	21.934	NEMO-3	[28]
^{100}Mo	5.8×10^{23}	23.763	NEMO-3	[28]
^{116}Cd	1.7×10^{23}	23.230	Solotvina	[29]
^{128}Te	7.7×10^{24}	24.886	Geochem.	[30]
^{130}Te	3.0×10^{24}	24.477	CUORICINO	[31]
^{136}Xe	4.5×10^{23}	23.653	DAMA	[32]

$$\mu < \frac{1}{2}(\gamma_i - \tau_i^{90}) - \eta_i < \frac{1}{2}(\gamma_i - \tau_i^{90}) - \eta_i^0 + 1.64\sigma_i = \mu^{90},$$
(18)

where we have linearly added two one-sided limits at 90%: an experimental one ($-\tau_i^{90}/2$) and a theoretical one ($-\eta_i^{90} + 1.64\sigma_i$). In the absence of more detailed information about the (unpublished) probability distribution of experimental τ_i's, this is the most conservative choice.

Figure 3 shows the results of this exercise, in terms of $m_{\beta\beta}/\text{eV} = 10^\mu$. The shaded band on the left corresponds to the 90% C.L. range in Eq. (15), while the bands on the right are obtained by inserting the τ_i^{90} limits of Table II into Eq. (18), except for the very weak limit from ^{96}Zr which is out of scale. No experiment appears to have probed the 90% C.L. range preferred by the Klapdor *et al.* claim, although IGEX and CUORICINO have almost reached its lower end.

It is affirmed in [31] that the CUORICINO limit probes part of the Klapdor *et al.* range in $m_{\beta\beta}$, seemingly in contrast with our results. However, the arguments in [31] involve a comparison of two *different* confidence levels, namely, the 90% C.L. limit from ^{130}Te versus the 99.73% C.L. range ($\pm 3\sigma$) from ^{76}Ge. The latter range is a factor
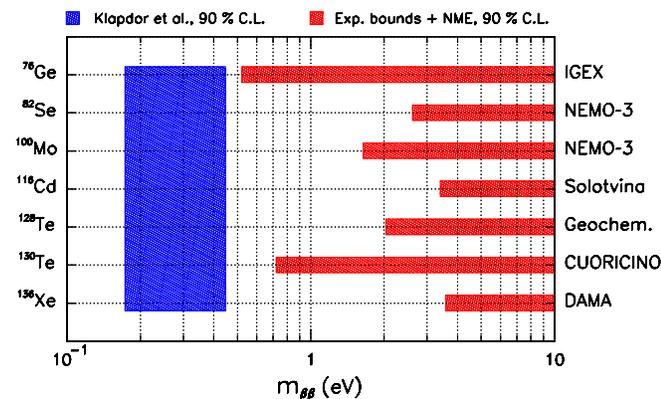

FIG. 3 (color online).   Range of $m_{\beta\beta}$ allowed at 90% C.L. by the $0\nu\beta\beta$ claim of [16], compared with the 90% limits placed by other experiments. The comparison involves the NME and their errors, as estimated in this work.

of $3\sigma/1.64\sigma = 1.83$ wider than the appropriate 90% C.L. range used in Fig. 3 (left side), and thus leads to more optimistic conclusions. In Ref. [14] the comparison was consistently made at the same C.L. for both nuclei, but it involved an intermediate step where correlations were not taken into account (see next subsection), leading again to an optimistic impact for the CUORICINO limit. The analysis proposed in this work shows that, actually, neither IGEX nor CUORICINO exclude fractions of the range claimed in [16] at comparable confidence levels, as far as our estimates for $\eta_i = \eta_i^0 \pm \sigma_i$ (and ρ_{ij}) hold.

B. Comparison of half-lives in a couple of nuclei

Here we consider a more direct comparison via observable half-lives in two nuclei, bypassing the unobservable Majorana mass $m_{\beta\beta}$. We take two different nuclei i and j, characterized by nuclear matrix elements $\eta_i = \eta_i^0 \pm \sigma_i$ and $\eta_j = \eta_j^0 \pm \sigma_j$ with correlation ρ_{ij}. A positive $0\nu\beta\beta$ signal in the first nucleus ($\tau_i = \tau_i^0 \pm s_i$) translates into a favored range for the second nucleus ($\tau_j = \tau_j^0 \pm s_j$) as follows.

From Eq. (10) one obtains, by difference,

$$\tau_j - \tau_i = \Delta_{ij} \pm \epsilon_{ij},$$
(19)

where

$$\Delta_{ij} \equiv \tau_j^0 - \tau_i^0 = (\gamma_j - \gamma_i) + 2(\eta_i^0 - \eta_j^0),$$
(20)

the error ϵ_{ij} being obtained by summing in quadrature the correlated uncertainties associated to the difference $2(\eta_i^0 - \eta_j^0)$,

$$\epsilon_{ij}^2 = 4(\sigma_i^2 + \sigma_j^2 - 2\rho_{ij}\sigma_i\sigma_j).$$
(21)

Note that, if the correlation term $-2\rho_{ij}\sigma_i\sigma_j$ were neglected, ϵ_{ij} would be overestimated. The error s_j associated to $\tau_j^0 = \tau_i^0 + \Delta_{ij}$ is obtained by summing in quadrature the uncorrelated errors s_i and ϵ_{ij},

$$s_i^2 = s_j^2 + \epsilon_{ij}^2.$$
(22)

As a result, the error s_j has a nonzero correlation r_{ij} with the error s_j, as given by $r_{ij}s_is_j = s_i^2$, namely,

$$r_{ij} = \frac{s_i}{s_j}.$$
(23)

If we apply the above results to $i = {}^{76}$Ge and $j = {}^{130}$Te, then the claim by Klapdor *et al.* in Eq. (14), $\tau_i = 25.355 \pm 0.072$, implies that $\tau_j = 24.786 \pm 0.161$, with error correlation $r_{ij} = 0.447$. Figure 4 shows the corresponding error ellipse at 1.64σ (90% C.L.), in the plane charted by the $0\nu\beta\beta$ half-lives of the nuclei $i = {}^{76}$Ge and $j = {}^{130}$Te. The ellipse can be thought as the combined result of two independent constraints, shown as 90% C.L. bands. The horizontal band corresponds to the experimental claim $\tau_i = 25.355 \pm (1.64 \times 0.072)$. The slanted band corre-
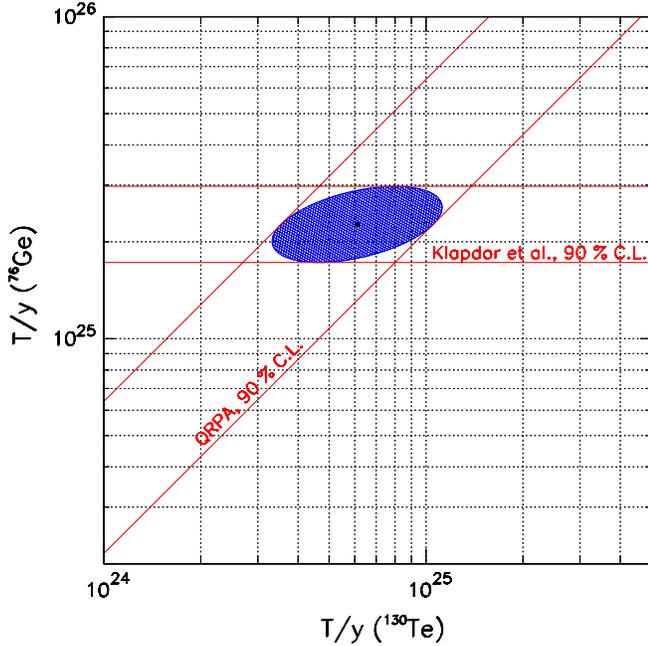
FIG. 4 (color online).   Example of theoretical and experimental constraints at 90% C.L., in the plane charted by the $0\nu\beta\beta$ half-lives of ^{76}Ge and ^{130}Te. Horizontal band: range preferred by the $0\nu\beta\beta$ claim of [16]. Slanted band: constraint placed by our QRPA estimates. The combination of the two constraints provides the shaded ellipse, whose projection on the abscissa gives the range preferred at 90% C.L. for the ^{130}Te half-life.

sponds to the theoretical limits placed by our QRPA estimates on the ratio T_j/T_i, namely, $\tau_j - \tau_i = \Delta \pm (1.64 \times \epsilon_{ij})$. Note that the projection of the ellipse on the x-axis provides the range preferred at 90% C.L. for the ^{130}Te half-life: $T_j/y = [0.33, 1.12] \times 10^{25}$. Projections for other nuclei can be similarly derived, as reported in Fig. 5.

Figure 5 shows the two-sided ranges preferred by the Klapdor *et al.* claim at 90% C.L. (shaded rectangles on the
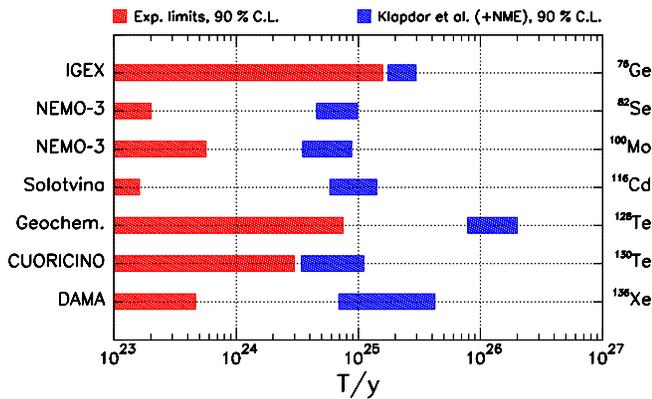

FIG. 5 (color online).   Range of half-lives T_i preferred at 90% C.L. by the $0\nu\beta\beta$ claim of [16], compared with the 90% limits placed by other experiments. The comparison involves the NME and their errors, as well as their correlations, estimated in this work.

right), as well as the one-sided 90% C.L. limits from Table II (bands on the left), for the same nuclei as in Fig. 3. The two-sided limits involve the use of NME errors and correlations, except for ^{76}Ge, which is a purely experimental input. Once more, we see that none of the existing limits can exclude a fraction of the range favored by Klapdor *et al.* [16] at a comparable confidence level, although IGEX and CUORICINO have almost reached it. The more optimistic claim about the CUORICINO impact in [31] was based on a larger favored range for the ^{130}Te half-life, as obtained by ignoring correlations in the ϵ_{ij} estimate of Eq. (21).

We emphasize that the contents of Figs. 3 and 5, although similar, are not equivalent. The comparison of experimental sensitivities in Fig. 3 is made in terms of a derived quantity ($m_{\beta\beta}$), while in Fig. 5 it is directly made in terms of observables (T_i). One-sided bounds in Fig. 3 are obtained by linearly adding 90% C.L. theoretical and experimental limits [Eq. (18)], while in Fig. 5 only the latter limits are used; conversely, theoretical errors are used with full correlation information in the allowed (two-sided) bars of Fig. 5. We think that a comparison in terms of observables, as in Fig. 5, provides a more faithful representation of the current $0\nu\beta\beta$ decay sensitivities.

We conclude this subsection by discussing the 90% C.L. prospective sensitivities (in terms of T_i) of the most promising future $0\nu\beta\beta$ projects. Table III reports such limits, according to the recent review in Ref. [26]. The values in Table III are largely beyond the two-sided favored ranges in Fig. 5, except perhaps for ^{136}Xe, where the expected sensitivity is only a factor <2 beyond the Klapdor *et al.* favored range. This gain may be insufficient if one requires a more demanding check of the claim, at a confidence level significantly higher than 90%. It should be added, however, that all the projects in Table III expect to proceed in a second phase of operation with larger exposures and lower backgrounds, improving the quoted sensitivities by, possibly, another order of magnitude [26].

C. Combination of half-life data from several nuclei, and degeneracy effects

Let us consider a future, optimistic situation where $0\nu\beta\beta$ decay is established in N different nuclei, with measured half-lives

TABLE III.   Prospective half-life sensitivities at 90% C.L. (T_i^{90}) for different nuclei i in promising future projects, as reported in [26].

i	T_i^{90}/y	Project
^{76}Ge	2.0×10^{26}	GERDA, MAJORANA
^{82}Se	2.0×10^{26}	SuperNEMO
^{130}Te	2.1×10^{26}	CUORE
^{136}Xe	6.4×10^{25}	EXO

$$\tau_i = \tau_i^0 \pm s_i \qquad (i = 1, \ldots, N). \qquad (24)$$

Assuming that $0\nu\beta\beta$ decays proceed only through light Majorana neutrino exchange, these measurements will fix one unknown parameter (μ) via a set of N linear equations analogous to Eq. (10),

$$\tau_i^0 \pm s_i = \gamma_i - 2(\eta_i^0 \pm \sigma_i) - 2\mu \qquad (i = 1, \ldots, N), \qquad (25)$$

where the experimental errors s_i are, in general, uncorrelated (being obtained in independent experiments), while the theoretical errors σ_i have nontrivial correlations ρ_{ij} (being obtained within the same QRPA model).

This overconstrained system can be solved by the least-squares method, i.e., by minimizing the χ^2 function

$$\chi^2(\mu) = \sum_{ij} (\tau_i^0 - \gamma_i + 2\eta_i^0 + 2\mu)$$
$$\times W_{ij}(\tau_j^0 - \gamma_j + 2\eta_j^0 + 2\mu), \qquad (26)$$

where the weight matrix W_{ij} is the inverse of the total covariance matrix (including experimental and theoretical errors),

$$[W]_{ij}^{-1} = \delta_{ij} s_i s_j + 4\rho_{ij}\sigma_i\sigma_j. \qquad (27)$$

The χ^2 function is quadratic in μ,

$$\chi^2(\mu) = a\mu^2 + b\mu + c, \qquad (28)$$

where

$$a = 4\sum_{ij} W_{ij}, \qquad (29)$$

$$b = 4\sum_{ij} W_{ij}(\tau_i^0 - \gamma_i + 2\eta_i^0), \qquad (30)$$

$$c = \sum_{ij}(\tau_i^0 - \gamma_i + 2\eta_i^0)W_{ij}(\tau_j^0 - \gamma_j + 2\eta_j^0). \qquad (31)$$

The minimum value $\chi^2_{\min}$ and the one-sigma shift $\chi^2_{\min} + 1$ are reached for $\mu = \mu_0$ and $\mu = \mu_0 \pm \delta$, respectively, where

$$\mu_0 = -\frac{b}{2a}, \qquad (32)$$

$$\delta = \frac{1}{\sqrt{a}}, \qquad (33)$$

$$\chi^2_{\min} = c - \frac{b^2}{4a}. \qquad (34)$$

The fit is acceptable if $\chi^2_{\min}/(N-1) \simeq 1$. Much higher value of $\chi^2_{\min}$ might signal, e.g., new physics beyond the standard mechanism of $0\nu\beta\beta$ decay via light Majorana neutrinos (barring experimental and theoretical mistakes). However, the analysis of nonstandard mechanisms is beyond the scope of this work.

As a practical example for the standard $0\nu\beta\beta$ case, we consider decay searches in each of the four nuclei reported in Table III, in the hypothesis that the true value of $m_{\beta\beta}$ is 0.2 eV (i.e., $\mu = -0.70$), close to the lower end of the range in Eq. (17). We assume that the experiments will measure the expected values for the half-lives T_i,

$$m_{\beta\beta}/\text{eV} = 0.2 \Rightarrow T_i/\text{y} = \begin{cases} 4.43 \times 10^{25} & (^{76}\text{Ge}), \\ 1.34 \times 10^{25} & (^{82}\text{Se}), \\ 1.20 \times 10^{25} & (^{130}\text{Te}), \\ 3.43 \times 10^{25} & (^{136}\text{Xe}), \end{cases} \qquad (35)$$

with a fractional uncertainty $\delta T_i/T_i = 20\%$ (corresponding to $s_i = 0.08$). By construction, the best fit to any combination of these mock data gives back $\mu_0 = -0.7$ and $\chi^2_{\min} = 0$. The relevant output parameter is then the reconstructed μ uncertainty, δ, from Eq. (33).

Table IV shows the δ values, for all possible combinations of mock data from the four nuclei (ranging from a single nucleus to all of them). We comment first the results in the 6th column, which are obtained by (incorrectly) switching off correlations, i.e., by setting $\rho_{ij} = \delta_{ij}$, as it is often done in the literature.

Without correlations, the error δ is given by the familiar combination of total errors from independent data,

$$\frac{1}{\delta^2} = \sum_i \frac{1}{\sigma_i^2 + (s_i/2)^2} \simeq \sum_i \frac{1}{\sigma_i^2}, \qquad (36)$$

where we have used the fact that any of the σ_i is a factor of 3–4 greater than $s_i/2 = 0.04$. Although the error δ is dominated by theoretical uncertainties, it decreases by

TABLE IV. Combination of any among the four hypothetical half-life data T_i in Eq. (35) with experimental uncertainty $\delta T_i/T_i = 20\%$. Results are given in terms of the total 1σ error δ on the parameter $\mu = \log_{10}(m_{\beta\beta}/\text{eV})$, including theoretical uncertainties without and with correlations. Bullets indicate the data included in the evaluation (from 1 to 4 data).

# of data	^{76}Ge	^{82}Se	^{130}Te	^{136}Xe	δ (w/o corr.)	δ (with corr.)
1	•				0.128	0.128
1		•			0.141	0.141
1			•		0.163	0.163
1				•	0.191	0.191
2	•	•			0.095	0.128
2	•		•		0.100	0.128
2	•			•	0.106	0.127
2		•	•		0.107	0.141
2		•		•	0.114	0.141
2			•	•	0.124	0.163
3	•	•	•		0.082	0.127
3	•	•		•	0.085	0.127
3	•		•	•	0.089	0.127
3		•	•	•	0.093	0.140
4	•	•	•	•	0.075	0.127

increasing the data sample (see 6th column of Table IV), as a consequence of (incorrectly) assuming no correlations. Formally, the combination of all the four data would then provide the estimate $\mu = -0.7 \pm 0.075$, corresponding to $m_{\beta\beta} \simeq 0.2 \pm 0.035$.

Unfortunately, including correlations spoils this nice result. Table IV (last column) shows that, with good approximation, the uncertainty δ cannot be much better than the smallest theoretical uncertainty σ_i among the set of nuclei included in the fit. Indeed, even with all four nuclei one obtains $\delta = 0.127$, nearly the same as $\delta = 0.128$ from the single nucleus ^{76}Ge (characterized by the smallest theoretical error, $\sigma_i = 0.122$). Therefore, regardless of how many accurate experiments are combined, the final accuracy for our test-case Majorana mass will not be better than $\mu \simeq -0.7 \pm 0.13$, namely, $m_{\beta\beta} \simeq 0.2 \pm 0.06$.

The degeneracy effect induced by correlations can be easily understood in the limiting case of equal and completely correlated theoretical errors ($\sigma_i \equiv \sigma$ and $\rho_{ij} \equiv \delta_{ij}$). In this case, the QRPA uncertainties would reduce to a common shift $\eta_i \rightarrow \eta_i + \delta$ for all nuclei, where $\delta \in [-\sigma, +\sigma]$ within one standard deviation. [In Fig. 1, the ellipses would collapse to "segments" with 45° slope in all panels.] A common shift of all η_i is degenerate with a shift $\mu \rightarrow \mu - \delta$ via Eq. (10),

$$\tau_i = \gamma_i - 2(\eta_i + \delta) - 2(\mu - \delta), \qquad (37)$$

and, thus, the parameter μ is affected by an irreducible uncertainty $\delta = \sigma$. For unequal NME errors σ_i, the most accurate one dominates in equations like Eq. (37) and thus

$$\delta \simeq \min\{\sigma_i\}, \qquad (38)$$

as anticipated.

The difference between δ estimates without or with correlations, in the combination of data from N different nuclei, is striking. Without correlations, and for comparable theoretical uncertainties, the error δ would scale as $\sqrt{N}$ [Eq. (36)]. Including correlations, the error δ becomes dominated by the single, most accurate NME, irrespective of N [Eq. (38)]. One should thus reduce not only the size, but also the correlations of theoretical errors, in order to fully exploit the $m_{\beta\beta}$ sensitivity of future, multiple-isotope $0\nu\beta\beta$ searches.

D. Prospective constraints on the absolute neutrino mass and Majorana phase

The Majorana mass in $0\nu\beta\beta$ decay ($m_{\beta\beta}$) is one of the most sensitive probes of the absolute neutrino mass scale m_ν, together with the effective neutrino mass in beta decay ($m_{\beta\beta}$) and the sum of the three neutrino masses in cosmology (Σ); see [14] for updated bounds. It is tempting to combine prospective data on ($m_{\beta\beta}$, m_β, Σ) in the optimistic case of a possible signal "waiting around the corner", i.e., for masses close to the current *conservative* cosmo-

logical bound $\Sigma \lesssim 0.6$ eV [14,34,35]:

$$m_1 \simeq m_2 \simeq m_3 \equiv m_\nu \simeq 0.2 \text{ eV}. \qquad (39)$$

For the sake of simplicity, within current neutrino oscillation phenomenology [14], we approximate the mixing matrix values U_{ei}^2 as:

$$U_{e1}^2 \simeq 0.69, \qquad (40)$$

$$U_{e2}^2 \simeq 0.31 e^{i\phi}, \qquad (41)$$

$$U_{e3}^2 \simeq 0, \qquad (42)$$

where ϕ is an unknown Majorana phase. For nearly degenerate masses it is thus [12]

$$m_\beta \simeq m_\nu, \qquad (43)$$

$$\Sigma \simeq 3m_\nu, \qquad (44)$$

$$m_{\beta\beta} \simeq m_\nu f, \qquad (45)$$

with

$$f \simeq |U_{e1}^2 + U_{e2}^2| \in [0.38, 1], \qquad (46)$$

where the upper (lower) end of the range is obtained for the *CP*-conserving case $e^{i\phi} = +1$ ($e^{i\phi} = -1$).

Let us test the above scenario with mock data, having the following central values and fractional 1σ errors:

$$m_\beta \simeq 0.2(1 \pm 0.5) \text{ eV}, \qquad (47)$$

$$\Sigma \simeq 0.6(1 \pm 0.3) \text{ eV}, \qquad (48)$$

$$m_{\beta\beta} \simeq 0.2(1 \pm 0.3) \text{ eV}. \qquad (49)$$

In the above equations, the 50% uncertainty on m_β corresponds to the smallest 1σ error estimated for the upcoming β-decay experiment KATRIN ($\delta m_\beta \simeq 0.1$ eV) [36]. A 30% uncertainty on Σ seems appropriate (and even conservative) for a signal in next-generation cosmological data [37,38]. The putative 30% uncertainty on $m_{\beta\beta}$ reflects the discussion in the previous subsection.

Combining the "data" in Eqs. (47) and (48), one obtains

$$m_\nu \simeq 0.2(1 \pm 0.25), \qquad (50)$$

which, together with Eq. (45) and the "datum" in Eq. (49), imply

$$f \simeq 1 \pm 0.4. \qquad (51)$$

This result, compared with the range in Eq. (46), would slightly prefer one *CP*-conserving case ($e^{i\phi} = +1$) over the other ($e^{i\phi} = -1$), at the level of $\sim 1.5\sigma$. Therefore, in an optimistic—but not completely unrealistic—scenario with degenerate neutrino masses, such as the one considered above, a possible determination of $m_\nu \sim 0.2$ eV with $\sim 25\%$ accuracy (via m_β plus Σ) might be accompanied by

some indications about the Majorana phase ϕ (via $m_{\beta\beta}$). In this sense, we feel sympathetic towards more encouraging viewpoints [39,40] than those expressed by a "no-go detection" for ϕ [41], although a real "measurement" of ϕ remains undoubtedly very challenging, even in the most favorable scenarios.

V. SUMMARY AND PROSPECTS

Nuclear matrix elements for $0\nu\beta\beta$ decay are affected by relatively large theoretical uncertainties. Within the QRPA approach, we have shown that, within a given set of nuclei, the correlations among NME errors are as important as their size. We have made a first attempt to quantify the covariance matrix of the NME, and to understand its effects in the comparison of current and prospective $0\nu\beta\beta$ results for two or more nuclei. The effects have been clarified through a series of examples, involving an increasing number of observables. It turns out that correlations may severely limit the accuracy in the reconstruction of $m_{\beta\beta}$ from any number of $0\nu\beta\beta$ observations in different nuclei, due to a degeneracy between NME and $m_{\beta\beta}$ uncertainties. In particular, the fractional error on $m_{\beta\beta}$ is ultimately dominated by a single fractional NME uncertainty (the smallest one, among the set of nuclei considered). Breaking correlations between different nuclei is thus an important goal, which requires constraining (and improving) the theoretical model of each nucleus by means of many independent data (not only $2\nu\beta\beta$ data as currently used). In this way, systematic effects common to all nuclei may be reduced. Another relevant goal is to compare correlation estimates in future independent calculations (e.g., QRPA versus shell-model). While pursuing such a long-term theoretical and experimental program, a covariance analysis like the one proposed in this work may represent a useful tool, in order to correctly estimate current or prospective sensitivities to $0\nu\beta\beta$ decay and to Majorana neutrino parameters.

APPENDIX

This Appendix clarifies the role of different conventions about the $0\nu\beta\beta$ phase-space factor G_i, the axial vector coupling g_A, the nuclear matrix elements M_i', and the nuclear radius R_{nucl}, in comparison with other authors.

An agreement on common conventions would be desirable in the future, to avoid possible confusion or ambiguity (see also [42]).

According to usual definitions, the phase-space G_i contains a factor $(g_A^2/R_{\text{nucl}})^2$, where $R_{\text{nucl}} = r_0 A^{1/3}$. In this work, the adopted values of G_i refer to $r_0 = 1.1$ fm and $g_A = 1.25$ [43], while changes of g_A are conventionally embedded in M_i' (rather than in G_i) via the prefactor $(g_A/1.25)^2$ in Eq. (4) [4,18]. In order to match such convention, alternative calculations of G_i using $r_0 = 1.2$ fm [44–46] must be rescaled by a factor $f_0^2 \simeq 1.2$ (where $f_0 \simeq 1.1 \simeq 1.2/1.1$) [42].

Table V compares three different phase-space calculations (in terms of $G_i m_e^2$), all normalized to the same reference values $g_A = 1.25$ and $r_0 = 1.1$ fm. One can notice residual differences of $\sim 5\%$ between the results of [43–45], and of $\sim 10\%$ between those of [43,46], presumably due to different approximations used to evaluate the electron wave function and the screening corrections. In our opinion, a typical uncertainty for the computed G_i values may be estimated as $\pm 5\%$, corresponding to a variation $\delta\gamma_i \simeq \pm 0.02$ for the γ_i values in Table I. Such minor error, being much smaller than the theoretical and experimental uncertainties considered in this work ($\delta\gamma_i \ll \sigma_i$, s_i), has been ignored—but it might become more important in the future.

Concerning the nuclear matrix elements $|M_i'|$, the values calculated in [22] (QRPA) and [23,24] (shell model) refer to $r_0 = 1.2$ fm, and must be rescaled by a factor $1/f_0$ for comparison with the NME used in this work. Furthermore, since the values in [22] do not embed the prefactor $(g_A/1.25)^2$, they must be rescaled by another factor 1.25^{-2} in the subcase $g_A = 1$; this further rescaling is not necessary for the NME values in [24]. Table VI reports the rescaled values of $|M_i'|$ from [22,24] (in terms of logarithms η_i), as also used in Fig. 2. These η_i values are all contained within our estimated three-standard-deviation ranges $\eta_i^0 \pm 3\sigma_i$, which are reported in the last two rows of Table VI.

TABLE V. Comparison of $G_i m_e^2$ estimates (in units of 10^{15} y^{-1}) for $g_A = 1.25$. The second column refers to the calculations reported in [43] for $r_0 = 1.1$ fm, as used in this work. The third and fourth columns refer to independent estimates [44–46] for $r_0 = 1.2$ fm, rescaled by a compensating factor $f_0^2 = 1.2$.

Nucleus	Ref. [43]	Refs. [44,45]	Ref. [46]
^{76}Ge	7.93	7.67	7.57
^{82}Se	35.2	33.8	32.8
^{96}Zr	73.6	70.2	68.4
^{100}Mo	57.3	54.8	52.8
^{116}Cd	62.3	59.3	56.2
^{128}Te	2.21	2.20	1.99
^{130}Te	55.4	53.2	49.7
^{136}Xe	59.1	56.8	52.4

TABLE VI. Estimates of $\eta_i = \log_{10}|M'_i|$ for each nucleus, as derived from the recent QRPA calculations in [22] (see Table I therein) and shell-model calculations in [24] (see Table 7 therein) after appropriate rescaling, in order to match the conventions used in this work. The estimates of [24] refer only to a subset of nuclei and to $g_A = 1.25$. The s.r.c. used (Jastrow or UCOM) are explicitly reported. The last two rows report the upper and lower ends of our three-standard-deviation ranges $\eta_i^0 \pm 3\sigma_i$ (for any s.r.c. and g_A), which embrace all the above η_i estimates.

Ref.	s.r.c.	g_A	^{76}Ge	^{82}Se	^{96}Zr	^{100}Mo	^{116}Cd	^{128}Te	^{130}Te	^{136}Xe
[22]	Jastrow	1.00	0.471	0.313	0.261	0.312	0.331	0.396	0.374	0.222
[22]	UCOM	1.00	0.582	0.427	0.400	0.451	0.435	0.531	0.501	0.335
[22]	Jastrow	1.25	0.564	0.401	0.274	0.396	0.441	0.488	0.435	0.271
[22]	UCOM	1.25	0.687	0.529	0.452	0.553	0.554	0.639	0.584	0.406
[24]	Jastrow	1.25	0.320	0.297				0.328	0.285	0.204
[24]	UCOM	1.25	0.407	0.380				0.418	0.382	0.299
This work	Lower limit at 3σ level		0.269	0.166	-0.703	0.017	-0.046	0.072	0.024	-0.307
This work	Upper limit at 3σ level		1.001	0.976	0.779	0.989	0.854	0.996	0.972	0.815

[1] F. T. Avignone III, S. R. Elliott, and J. Engel, Rev. Mod. Phys. **80**, 481 (2008).

[2] C. Amsler *et al.* (Particle Data Group), Phys. Lett. B **667**, 1 (2008).

[3] A. Faessler and F. Šimkovic, J. Phys. G **24**, 2139 (1998).

[4] V. A. Rodin, A. Faessler, F. Simkovic, and P. Vogel, Nucl. Phys. **A766**, 107 (2006); **A793**, 213(E) (2007).

[5] K. Zuber, in *Summary of the Workshop on Nuclear matrix elements for neutrinoless double beta decay presented at IPPP* (University of Durham, Durham, England, 2005).

[6] S. M. Bilenky and J. A. Grifols, Phys. Lett. B **550**, 154 (2002).

[7] S. M. Bilenky, C. Giunti, J. A. Grifols, and E. Masso, Phys. Rep. **379**, 69 (2003).

[8] S. M. Bilenky and S. T. Petcov, arXiv:hep-ph/0405237.

[9] F. Simkovic, Prog. Part. Nucl. Phys. **57**, 185 (2006).

[10] F. Deppisch and H. Pas, Phys. Rev. Lett. **98**, 232501 (2007).

[11] V. M. Gehman and S. R. Elliott, J. Phys. G **34**, 667 (2007); **35**, 029701(E) (2008).

[12] G. L. Fogli, E. Lisi, A. Marrone, A. Melchiorri, A. Palazzo, P. Serra, and J. Silk, Phys. Rev. D **70**, 113003 (2004).

[13] G. L. Fogli *et al.*, Phys. Rev. D **75**, 053001 (2007).

[14] G. L. Fogli *et al.*, Phys. Rev. D **78**, 033010 (2008).

[15] H. V. Klapdor-Kleingrothaus, I. V. Krivosheina, A. Dietz, and O. Chkvorets, Phys. Lett. B **586**, 198 (2004).

[16] H. V. Klapdor-Kleingrothaus and I. V. Krivosheina, Mod. Phys. Lett. A **21**, 1547 (2006).

[17] G. D'Agostini, arXiv:physics/0403086.

[18] F. Simkovic, A. Faessler, V. Rodin, P. Vogel, and J. Engel, Phys. Rev. C **77**, 045503 (2008).

[19] F. Simkovic, A. Faessler, and P. Vogel, Phys. Rev. C **79**, 015502 (2009).

[20] J. P. Schiffer *et al.*, Phys. Rev. Lett. **100**, 112501 (2008); B. P. Kay *et al.*, arXiv:0810.4108.

[21] D. Frekers, Prog. Part. Nucl. Phys. **57**, 217 (2006); H. Dohmann *et al.*, Phys. Rev. C **78**, 041602 (2008); E. W. Grewe *et al.*, Phys. Rev. C **78**, 044301 (2008).

[22] J. Suhonen and M. Kortelainen, Int. J. Mod. Phys. E **17**, 1 (2008).

[23] J. Menendez, A. Poves, E. Caurier, and F. Nowacki, arXiv:0801.3760.

[24] J. Menendez, A. Poves, E. Caurier, and F. Nowacki, arXiv:0809.2183.

[25] A. Faessler, G. L. Fogli, E. Lisi, V. Rodin, A. M. Rotunno, and F. Simkovic, J. Phys. G **35**, 075104 (2008).

[26] A. S. Barabash, Talk at the 13th Lomonosov Conference on Elementary Particle Physics (Moscow, Russia, 2007).

[27] C. E. Aalseth *et al.* (IGEX Collaboration), Phys. Rev. D **65**, 092007 (2002).

[28] A. S. Barabash, in *Proceedings of ICHEP'06, 33rd International Conference on High Energy Physics 2006*, edited by A. Sissakian, G. Kozlov, and E. Kolganova (World Scientific, Moscow, Russia, 2007), p. 276; A. S. Barabash for the (NEMO Collaboration), talk at *NPAE 2008, 2nd International Conference on Current Problems in Nuclear Physics and Atomic Energy* (Kyiv, Ukraine, 2008).

[29] F. A. Danevich *et al.*, Phys. Rev. C **68**, 035501 (2003).

[30] T. Bernatowicz, J. Brannon, R. Brazzle, R. Cowsik, C. Hohenberg, and F. Podosek, Phys. Rev. C **47**, 806 (1993).

[31] C. Arnaboldi *et al.* (CUORICINO Collaboration), Phys. Rev. C **78**, 035502 (2008).

[32] R. Bernabei *et al.*, Phys. Lett. B **546**, 23 (2002).

[33] H. V. Klapdor-Kleingrothaus *et al.*, Eur. Phys. J. A **12**, 147 (2001).

[34] E. Komatsu *et al.* (WMAP Collaboration), arXiv:0803.0547.

[35] F. De Bernardis, P. Serra, A. Cooray, and A. Melchiorri, Phys. Rev. D **78**, 083535 (2008).

[36] E. W. Otten and C. Weinheimer, Rep. Prog. Phys. **71**, 086201 (2008).

[37] S. Hannestad and Y. Y. Y. Wong, J. Cosmol. Astropart. Phys. 07 (2007) 004.

[38] J. Lesgourgues and S. Pastor, Phys. Rep. **429**, 307 (2006).

[39] S. Pascoli, S. T. Petcov, and T. Schwetz, Nucl. Phys. **B734**, 24 (2006).

[40] F. Deppisch, H. Pas, and J. Suhonen, Phys. Rev. D **72**, 033012 (2005).

[41] V. Barger, S. L. Glashow, P. Langacker, and D. Marfatia, Phys. Lett. B **540**, 247 (2002).

[42] S. T. Cowell, Phys. Rev. C **73**, 028501 (2006).

[43] F. Simkovic, G. Pantis, J. D. Vergados, and A. Faessler, Phys. Rev. C **60**, 055502 (1999).

[44] M. Doi, T. Kotani, and E. Takasugi, Prog. Theor. Phys. Suppl. **83**, 1 (1985).

[45] F. Bohem and P. Vogel, *Physics of Massive Neutrinos* (Cambridge University Press, Cambridge, UK, 1992), p. 249.

[46] J. Suhonen and O. Civitarese, Phys. Rep. **300**, 123 (1998).